Characterization of hydrological response of the Dawen River Basin under land use change

Yanling Luo
Shandong Agricultural University
Xinhe Qiao
Shandong Agricultural University
Yunlong Dong
Shandong Agricultural University
Zhonglun Feng
Shandong Agricultural University
Jie Zhang
Shandong Agricultural University
Gang Wang
gwang@sdau.edu.cn
Shandong Agricultural University

Article

Keywords:

Posted Date: June 28th, 2024

DOI: https://doi.org/10.21203/rs.3.rs-4568222/v1

Additional Declarations: No competing interests reported.

Characterization of hydrological response of the Dawen River Basin under land use change

Yanling Luo 1, Xinhe Qiao 1, Yunlong Dong 1, Zhonglun Feng 1, Jie Zhang 1, and Gang Wang 1，*

[1] College of Water Conservancy and Civil Engineering, Shandong Agricultural University , Tai'an，271018, China

* gwang@sdau.edu.cn

Abstract

Land use change is one of the dominant drivers of hydrological change in the basin. Assessing the hydrological responses to land use changes is crucial for sustainable water resource management. We focused on the Dawen River Basin to analyze land use dynamics from 1985 to 2021. Using the SWAT model, we assessed hydrological responses under various land use scenarios, quantified impacts on hydrological elements, and employed the Random Forest Method to evaluate the impact of different land use types on runoff. Results show that from 1985 to 2021, cropland and grassland in the watershed decreased by 11.57% and 52.04%, respectively, while forest land and construction land increased by 11.45% and 103.85%, respectively; other land types showed no significant changes. These land use changes resulted in an increase in watershed evapotranspiration by 26.53 mm, a decrease in groundwater recharge by 19.64 mm, and an increase in surface runoff depth by 18.94 mm. Cultivated land, forest land, and grassland were identified as the major influencers on watershed runoff, with importance weights of 1.0729, 0.9607, and 0.8305, respectively. The variations in hydrological elements within the Dawen River watershed during the study period were primarily associated with the reduction in cultivated land and grassland area, coupled with an increase in constructed land area.

Introduction

The acceleration of global climate change and urbanization has led to significant changes in hydrological elements such as basin precipitation, runoff, and evapotranspiration. These changes have increased the variability and diversity of basin hydrological processes, posing challenges to the management of water resources and sustainable development efforts[1]. The scientific identification of the impacts of various driving factors on basin hydrology has been a key focus of the International Association of Hydrological Sciences (IAHS) initiative 'Panta Rhei - everything flows' from 2013 to 2022 [2,3]. Among these factors, land use change has emerged as a critical area of study within the broader field of global environmental change [4-6].

Land use change encompasses alterations in the ways and types of land use, including the transformation of natural landscapes for human purposes and changes in managed land practices[7]. These changes, by modifying conditions such as surface roughness, vegetation cover, and soil infiltration characteristics, trigger alterations in climate, soil, hydrology, and geomorphology within a watershed. Such modifications influence the mechanisms of runoff generation, convergence, and water distribution [8-10]. Furthermore, changes in surface conditions can lead to short-term hydrological changes, while long-term activities like urbanization and deforestation may result in weakened evapotranspiration and alterations in water cycle

dynamics. Land use change is a complex and spatiotemporally variable process that has enduring impacts on watershed hydrology[11-14].

The primary methods for quantitatively analyzing the impact of land use change on watershed hydrology are the paired watershed method, time series analysis, and hydrological modeling[15-17]. Implementing the paired watershed method is challenging due to difficulties in finding two similar medium or large-sized watersheds, which may also undergo significant changes at different stages, thereby limiting its practical application[18]. Time series analysis allows for the examination of trends in hydrological and climatic data of watersheds; however, the spatial heterogeneity of watersheds and the interactions between land use/land cover changes and climate change effects on the water cycle remain uncertain. Since the 1970s, advancements in computer science, geographic information systems, and remote sensing technology have enhanced hydrological models as effective tools for assessing hydrological responses to environmental changes. Among these, the SWAT model stands out for its suitability and effectiveness in simulating hydrological responses to land use/land cover changes [19,20]. SWAT provides detailed simulations of hydrological processes[21]and exhibits superior runoff simulation capabilities compared to other models[22]. It is extensively used across Europe, North America, Australia, Africa, and other regions[23-25].Zhang et al[26] utilized an improved SWAT model to simulate the hydrological processes in the North Johnstone River Basin, finding that urbanization increased surface runoff while decreasing lateral flow and groundwater recharge. Additionally, afforestation was shown to decrease surface runoff and soil moisture, while increasing evapotranspiration. In another study, Zhang et al[27] employed the SWAT model to explore the effects of land use changes on runoff mechanisms and rainfall infiltration coefficients in the Beijing-Su-Mi-Huai region. They integrated MODFLOW to analyze the water balance of the area during typical hydrological years. The results showed that between 2000 and 2015, the transformation of plain farmland into construction land increased runoff by 7 × 10^6 m³ and raised the runoff coefficient by 17.9%. Furthermore, Hu et al[28] examined spatiotemporal land use changes in the Weihe River Basin from 1980 to 2010, across four regions and three landform types. They quantified the spatial heterogeneity of hydrological responses to different land use changes based on their analysis.

The Dawen River, the largest tributary of the Yellow River within Shandong Province, China, is characterized by its relatively abundant natural water resources compared to the rest of the region. This study focuses on the Dawen River Basin, employing hydrological modeling to quantitatively analyze the impacts of land use changes on watershed hydrological elements from 1985 to 2021. The objective is to provide a scientific basis for the development and management of water and soil resources in the basin. The main research topics include: (1) analyzing and compiling statistics on the spatial characteristics of land use types in the Dawen River Basin, along with changes in land use types from 1985 to 2021; (2) constructing a SWAT model to quantitatively assess the impact of these changes on hydrological elements; (3) investigating the causes of variability in surface runoff and quantifying how different land use types influence it.

Methods

Study Area

Located in the central part of Shandong Province, China, the Dawen River Basin forms part of the Yellow River Basin (refer to Figure 1). The basin's topography gradually declines from east to west and from north to south, broadening in the east and narrowing in the west. It is bounded to the north by Mount Tai and flanked to the east by the Lushan and Mengshan Mountains, with hills and plains characterizing the

western and southern regions. The basin's diverse terrain includes 31% mountainous areas, 37% hilly regions, and hills that rise above 300 meters making up one-sixth of its total area. The soil types within the basin are varied, comprising brown soil, alluvial soil, sandy soil, loamy black soil, and mountain grassland soil, with the latter primarily found at elevations above 1200 meters in the Mount Tai area. Additional sandy soil patches are located west of Dongping Lake. The region is classified within the warm temperate broad-leaved forest zone, with its natural vegetation being relatively sparse in the mountainous areas, which contributes to severe soil erosion. The predominant flora includes pine and cypress in the uplands, while shrubs dominate the lower hilly areas. The plains host plantations of phoenix trees and willows. The basin supports a substantial amount of arable land, mainly cultivated with wheat and corn, alongside extensive orchards and vegetable gardens. A smaller portion of the land supports the cultivation of cash crops like cotton, garlic, and ginger.

The Dawen River exhibits an average annual runoff of approximately 1.82 billion cubic meters, with the majority, about 64%, occurring in July and August. The historical peak of annual runoff reached 6.07 billion cubic meters in 1964, contrasting sharply with a record low of 500 million cubic meters in 1968. The climate within the basin is characterized by mild temperatures and plentiful rainfall, although precipitation distribution is notably uneven. The bulk of the rainfall, accounting for 75% of the annual total, occurs between June and September.

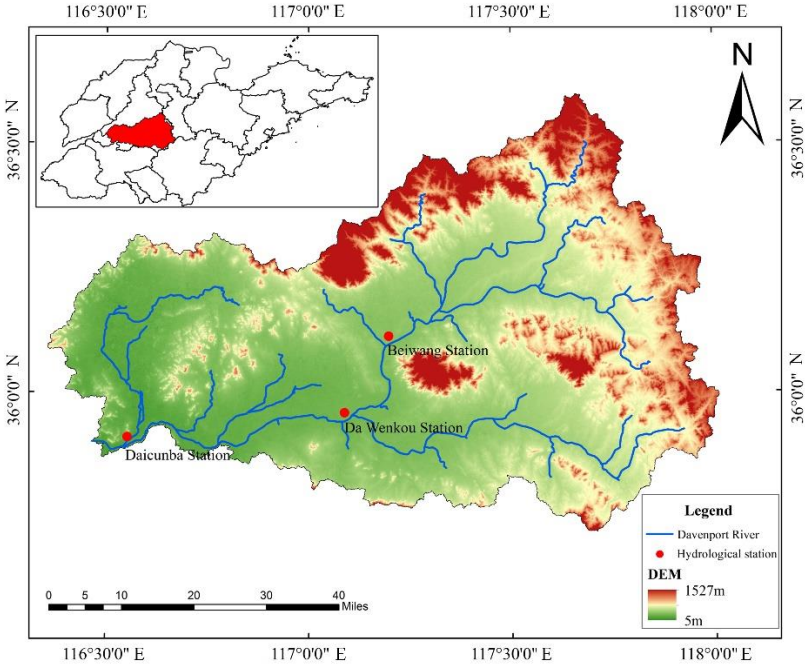

Figure 1. Location Map of the Dawen River Basin (Upper Dawen River at Daicun Dam)

Data and Sources

Hydrological model establishment requires the following data:DEM (Digital Elevation Model) data; Land use data; Soil type distribution and attribute data; Meteorological data and Streamflow data

Soil textures vary in their permeability and absorption rates, significantly influencing the capabilities for rainfall infiltration and runoff generation. For modeling purposes, detailed soil maps and a database containing characteristics of different soil layers—such as hydrological groups, maximum rooting depths, and bulk densities—are essential. In this study, the Harmonized World Soil Database (HWSD) was

utilized to extract relevant soil data for the basin. Soil types within the study area were reclassified, and soil parameters recalculated. Cambisol, the predominant soil type, covers 51.58% of the area and is crucial for agricultural production. The next most prevalent soil types, Regosol and Lithosol, collectively constitute about 40% of the study area.

Precipitation and temperature are fundamental variables in the global water cycle and surface hydrological processes, serving as key factors in hydrological, meteorological, and ecological studies. These elements are crucial for influencing runoff, as noted in recent research[29,30]. For this study, the China Meteorological Assimilation Driving Datasets for the SWAT Model (CMADS) were chosen due to their extensive coverage and high resolution, making them a popular tool among researchers for hydrological model simulations. We utilized CMADS to establish the meteorological database for our model, selecting data from 24 meteorological stations within and around the study area. The data, spanning from 2008 to 2018, were processed and formatted to be compatible with the SWAT model.

Runoff data for this study were sourced from three key hydrological stations within the basin: Daicun Dam Station, Dawenkou Station, and Beiwang Station, as depicted in Figure 1. We utilized monthly runoff data spanning from 2008 to 2013 to calibrate and validate the model.

Construction of the SWAT Model

The SWAT model, developed by Dr. Jeff Arnold[31,32] of the United States Department of Agriculture Agricultural Research Service is a distributed hydrological model used to simulate various physical processes occurring within a watershed. These processes are driven by water balance. The model mainly consists of hydrological process sub-models, soil erosion sub-models, and pollution loading sub-models. When simulating surface runoff in the watershed, SWAT often adopts the SCS runoff curve method. The SCS curve number method is a research result concerning the precipitation-runoff relationship. It provides a basis for estimating runoff under various soil and land use types. The specific equation is as follows：

$$\mathbf{Q}_{surf} = \frac{(\boldsymbol{R_{day}-I_a})^2}{(\boldsymbol{R_{day}-I_a+S})} \qquad (1)$$

Q_{surf} represents the cumulative surface runoff, measured in millimeters (mm); R_{day} represents the rainfall depth on a certain day, measured in millimeters (mm); I_a represents the initial loss, which includes depression storage, interception by vegetation, and infiltration, measured in millimeters (mm);S represents the curve number.

The water balance is the foundation of model operation. The water balance equation used in the model is as follows:

$$\mathbf{SW_t} = \boldsymbol{SW_0} + \sum_{\boldsymbol{i=1}}^{\boldsymbol{t}}(\boldsymbol{R_{day} - Q_{surf} - E_a - W_{seep} - Q_{gw}}) \qquad (2)$$

SW_t represents the final soil moisture content on day *i*, measured in millimeters (mm);SW_0 represents the initial soil moisture content on day *i*, measured in millimeters (mm);t represents time;R_{day} represents the precipitation on day *i*, measured in millimeters (mm);Q_{surf} represents the surface runoff on day *i*, measured in millimeters (mm);E_a represents the evapotranspiration on day *i*, measured in millimeters (mm);W_{seep} represents the percolation and lateral flow of soil layers on day *i*, measured in millimeters (mm);Q_{gw} represents the groundwater content on day *i*, measured in millimeters (mm).

The SWAT model calculates by dividing the watershed into sub-basins and introducing Hydrological Response Units (HRUs) to replace grids. Sub-basins are formed when the cumulative flow accumulation

into the river grid unit exceeds the threshold of the watershed area. HRUs are one of the distinguishing features of the SWAT model and represent the smallest units for flow routing and water balance calculations. They refer to homogeneous areas with uniform underlying surfaces, reflecting spatial heterogeneity in terms of different land use types, soil types, and slope combinations. In this study, based on watershed DEM data, a watershed area threshold of 8500 hm^2 was set, dividing the study area into 67 sub-basins and 528 HRUs. To accurately analyze the response of watershed hydrological elements to land use changes, the thresholds for land use type units were set to 0, while those for soil type and slope were set to 10% and 5%, respectively.

Model Calibration and Validation

SWAT-CUP is an independent computer program developed for the calibration, validation, and uncertainty analysis of SWAT. It is used to optimize SWAT model parameters[33]. SWAT-CUP links five different calibration procedures, which are Sequential Uncertainty Fitting Ver. 2 (SUFI-2)[34], Generalized Likelihood Uncertainty Estimation (GLUE)[35], Particle Swarm Optimization (PSO)[36], Parameter Solution (ParaSol)[37], and Markov Chain Monte Carlo (MCMC)[38].The SUFI-2 program is highly effective for large-scale models that are time-consuming[39]. Therefore, in this study, the SUFI-2 program was chosen for model calibration and validation. Global sensitivity analysis was conducted to obtain parameter value ranges and sensitivity rankings, as shown in Table 1.

Table 1. Parameter sensitivity analysis

Typology	Sensitivity parameters	Hidden meaning	Range of values	Sensitivity ranking
Runoff	CN2	SCS runoff curve number	-0.2~0.2	1
	SURLAG	Surface runoff lag time	0.05~24	7
Evaporation	ESCO	Soil evaporation compensation factor	0.1~1	6
Soil	SOL_AWC	Soil available water capacity	0~1	9
Main river channel	CH_N2	The Manning coefficient for the main channel	-0.01~0.3	3
	CH_K2	The effective hydraulic conductivity of the main channel bed	-0.01~500	5
Baseflow	ALPHA_BF	Baseflow recession coefficient	0~1	2
	GW_DELAY	Groundwater delay coefficient	30~450	8
	GWQMN	Parameters for shallow groundwater runoff	0~5000	4

The simulated runoff results were compared and validated using measured runoff data from three hydrological stations: Daicun Dam, Dawenkou, and Beiwang. The measured runoff data for the Daicun Dam station are available from 2008 to 2016. However, all three stations experienced varying degrees of data loss from 2014 to 2016. Due to these limitations in runoff data, the period from 2008 to 2011 was selected as the calibration period for the model simulations, while the period from 2012 to 2013 was chosen for validation. Consistency was maintained between the calibration and validation periods for all three hydrological stations.

The coefficient of determination, R^2, is a metric used to evaluate the correlation between simulated and observed values in a model. It represents the consistency of the simulated values with the observed values. The closer the value of R^2 is to 1, the more closely the simulated values match the observed values. Typically, an R^2 value greater than 0.6 is considered as the standard for the correlation between observed and simulated values.

$$R^2 = \frac{\left[\sum_{t=1}^{n}(Q_{m,i} - \overline{Q_m})(Q_{s,i} - \overline{Q_s})\right]^2}{\sum_{t=1}^{n}(Q_{m,i} - \overline{Q_m})^2 \sum_{t=1}^{n}(Q_{s,i} - \overline{Q_s})^2} \quad (3)$$

$Q_{m,i}$ represents the observed runoff values, $\overline{Q_m}$ represents the mean of observed runoff values, $Q_{s,i}$ represents the modeled runoff values, $\overline{Q_s}$ represents the mean of modeled runoff values,and n represents the length of the observed time series.

The Nash-Sutcliffe Efficiency (NSE) is a normalized statistical index that determines the variance of residuals between observed and modeled values. It indicates the deviation between observed and modeled values and is one of the most commonly used standards for comparing hydrological model simulations with observed data. The closer its value is to 1, the smaller the deviation between the simulated and observed values, indicating higher reliability. When NSE≤0.36, the simulation performance is considered poor. When 0.36 < NSE <0.75 the simulation performance is considered satisfactory. When NSE≥0.75, the simulation results are considered good[40]. The formula for calculating the Nash-Sutcliffe Efficiency is as follows:

$$E_{NS} = 1 - \frac{\sum_{t=1}^{n}(Q_m - Q_0)^2}{\sum_{t=1}^{n}(Q_m - \overline{Q_m})^2} \quad (4)$$

Q_m represents the observed flow, Q_0 represents the simulated flow, and $\overline{Q_m}$ represents the multi-year average observed flow.

Random Forest Algorithm

The Random Forest algorithm is a fusion algorithm based on decision tree classifiers. Random Forest regression, on the other hand, is an algorithm based on ensemble learning, which performs the regression task by constructing multiple decision trees and integrating their predictions[41]. In a random forest, each decision tree is independent and trained on a randomly selected subsample, which effectively reduces the risk of overfitting. Random forests obtain the final regression results by averaging or weighted averaging the predictions of multiple decision trees. This ensemble approach helps to improve prediction accuracy and generalization.

Results

Model Applicability Analysis

Figure 2 illustrates the monthly-scale simulated runoff results for the calibration and validation periods at the Daicun Dam, Dawenkou, and Beiwang stations. It can be observed from the figure that runoff in the watershed is positively correlated with precipitation. During both the calibration and validation periods, the simulated monthly-scale runoff values at each hydrological station closely match the observed values, showing consistent trends. Based on the model evaluation results, the coefficient of determination ($R^{2)}$ and Nash-Sutcliffe Efficiency (NSE) for each station during the calibration period are both greater than

0.7. During the validation period, both R^2 and NSE values exceed 0.9, meeting the accuracy requirements of the model.

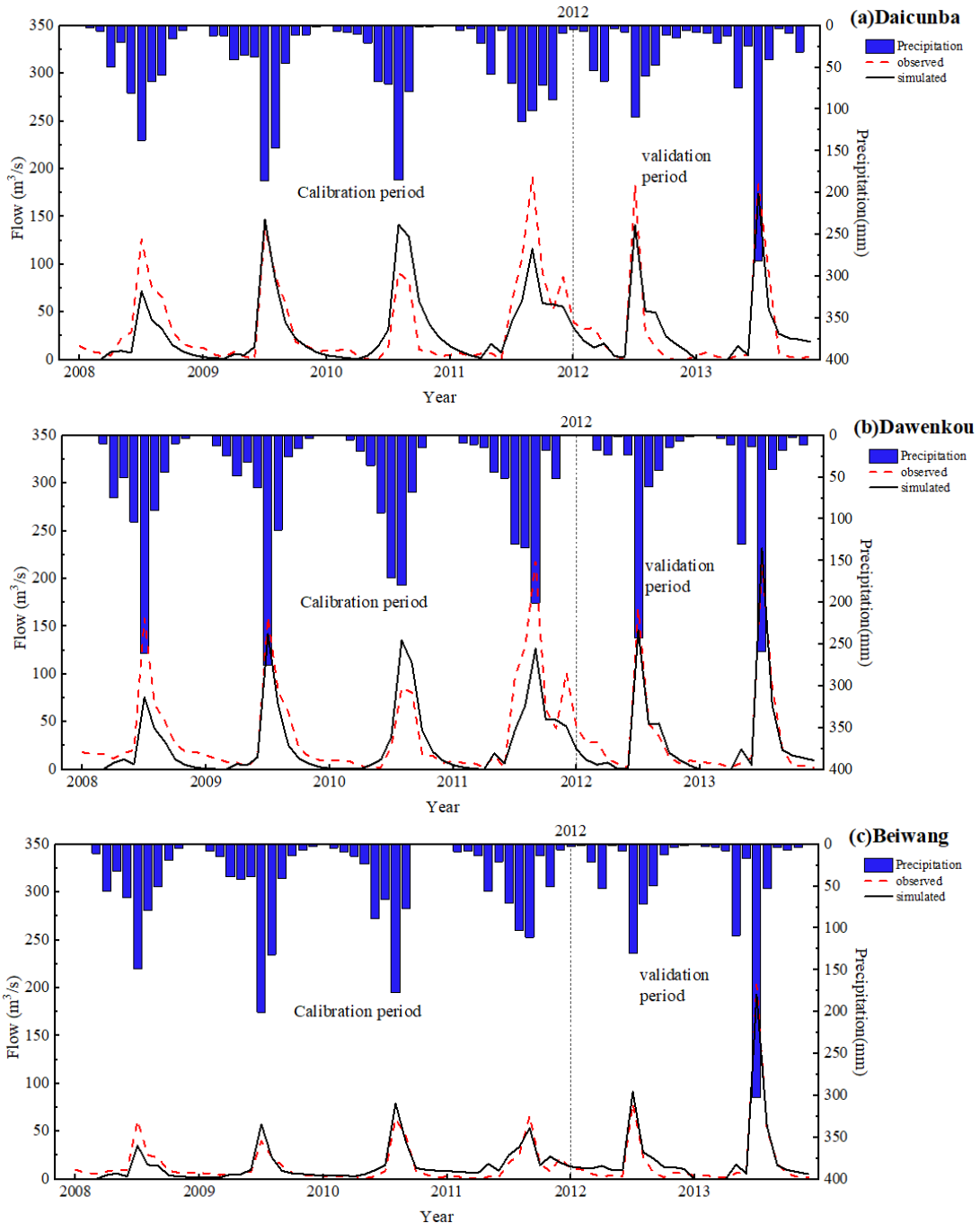

Figure 2. Measured and modelled monthly runoff values at hydrological stations

Analysis of Land Use Change

Figure 3 depicts the spatial distribution of land use types in the Dawen River Basin in 1985, 2005, and 2021. It can be observed that the overall spatial distribution of land use in the Dawen River Basin from

1985 to 2021 did not change significantly. Arable land, forest land, and grassland are widespread, with arable land being the predominant type, evenly distributed and extending across all parts of the study area.Arable land and urban construction land are mainly concentrated in the plain areas in the western and central parts of the basin, adjacent to rivers, lakes, and other water bodies. Forests and grasslands are primarily located in the northeastern hilly and mountainous areas, with grasslands mostly found at the edges of forested areas. Unutilized land types are scattered in the mountainous areas where the land is not cleared.

Table 2 presents the changes in land use in the Da Wen River Basin during the period from 1985 to 2021. From 1985 to 2021, the area of cropland and grassland decreased by 11.57% and 11.04% respectively, while the area of forestland, water bodies, and built-up areas increased by 11.45%, 111.5%, and 103.85% respectively. Although the area of forestland decreased between 1985 and 2005, it showed an overall increasing trend.

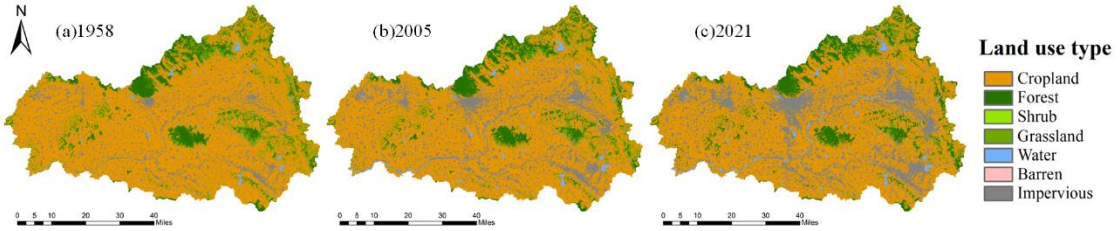

Figure 3. The land use type distribution in the Da Wen River Basin in 1985, 2005, and 2021

Table 2. Changes in land use types over different periods

Land use type	Area（km2)			Rate of change in area(%)		
	1985	2005	2021	1985-2005	2005-2021	1985-2021
Cropland	5988.81	5652.60	5296.02	-5.61	-6.31	-11.57
Forest	705.59	699.76	786.35	-0.83	12.37	11.45
Shrub	1.25	0.16	0.26	-87.05	60.60	-79.20
Grassland	696.72	495.26	334.17	-28.92	-32.53	-52.04
Water	59.20	115.43	125.21	94.98	8.47	111.50
Barren	2.66	0.39	0.26	-85.35	-32.85	-90.16
Impervious	841.08	1300.68	1714.53	54.64	31.82	103.85

Figure 4 illustrate the structure of land use and transfers over time. Against the backdrop of accelerated urban economic development and urbanization, cropland has become the main source of new expanded built-up areas. Under the policy of returning farmland to forest and grassland, some cropland has been converted into forestland and grassland. However, at the same time, the conversion of grassland to cropland has been significantly stronger than the progress of returning farmland to grassland and returning forestland to grassland projects, leading to a continuous decrease in grassland area and serious degradation of grasslands. Overall, from 1985 to 2021, there have been no significant changes in the overall proportion of land use types in the basin, with cropland remaining the dominant land use type.

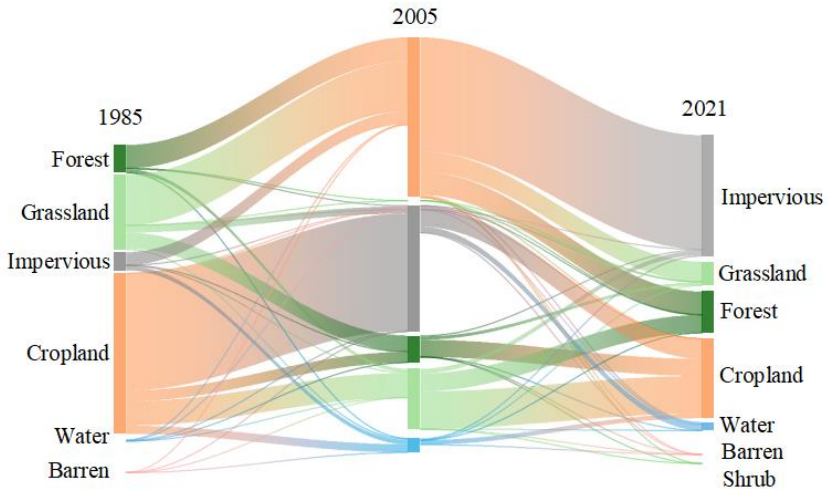

Figure 4. Transitions of land use types over different periods

Analysis of the response of hydrological elements to land use changes

After inputting land use data from 1985, 2005, and 2021 into the SWAT model, we calculated the average monthly and seasonal surface runoff depths for the basin across various land use scenarios, as illustrated in Figure 5. Under different land use scenarios, the temporal variation of surface runoff depth in the basin exhibits consistency, characterized by uneven distribution throughout the year, distinct boundaries between wet and dry seasons, and significant seasonal differences. The average monthly runoff depth was 11.21 mm under the 1985 land use scenario and increased to 12.79 mm by the 2021 scenario, reflecting an increase of 1.58 mm or 14.09%. Among various months, March exhibited the largest variation in runoff, whereas January had the least. Considering the monthly distribution of runoff and seasonal differences, it is evident that land use has a stronger regulatory effect on runoff during the wet season compared to the dry season.

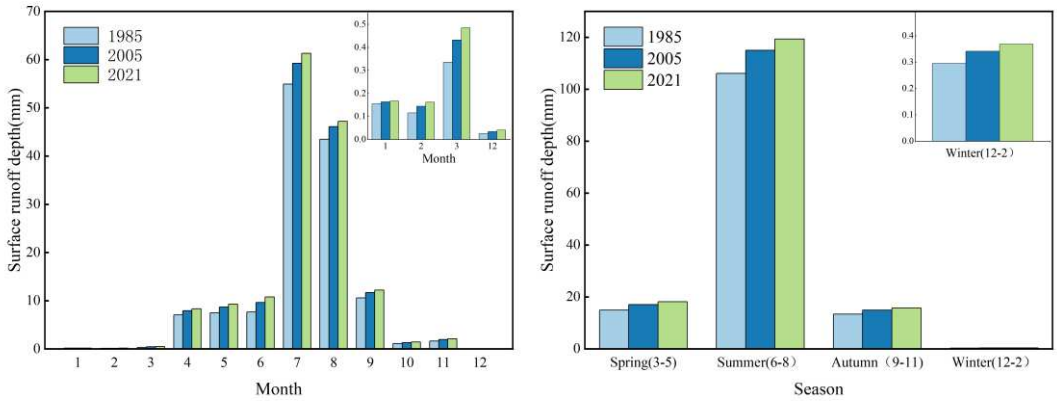

Figure 5. Average monthly and seasonal surface runoff depth over different periods

The results for the annual average evapotranspiration, groundwater recharge, surface runoff depth, and soil moisture under different land use scenarios across the entire basin are presented in Table 3. The

trends in hydrological elements are consistent across the three periods. From 1985 to 2005, groundwater recharge decreased by 13.25 mm, while surface runoff depth increased by 12.69 mm. During this period, the changes in land use were mainly characterized by a reduction in cropland, grassland, and forestland areas. The decrease in vegetation cover limited the vegetation's water retention and conservation functions, resulting in inhibited surface water infiltration, decreased groundwater recharge, and increased surface runoff. Additionally, the increase in built-up areas led to an increase in impervious surfaces, further inhibiting surface water infiltration and promoting surface runoff. From 2005 to 2021, evapotranspiration increased by 7.88 mm, primarily due to an increase in forestland area. Although the areas of cropland and grassland decreased compared to 2005, forests have higher transpiration rates than other vegetation types. Moreover, the increase in water bodies also contributed to the promotion of evapotranspiration. Based on the water balance, with increased evapotranspiration, decreased groundwater recharge, and increased surface runoff, soil moisture is expected to decrease, consistent with the model simulation results.

Table 3. Changes in various hydrological elements across different periods in the basin

Hydrological elements	Annual mean(mm)			Change(mm)		
	1985	2005	2021	1985-2005	2005-2021	1985-2021
ETmm	260.89	279.54	287.42	18.65	7.88	26.53
GW_Qmm	162.98	149.73	143.34	-13.25	-6.40	-19.64
SURQmm	134.56	147.26	153.50	12.69	6.25	18.94
SWmm	799.63	789.47	777.02	-10.16	-12.45	-22.62

Overall, during the study period, changes in land use types in the Da Wen River Basin resulted in an increase of 26.53 mm in evapotranspiration, a decrease of 19.64 mm in groundwater recharge, an increase of 18.94 mm in surface runoff depth, and a decrease of 22.62 mm in soil moisture. The main reasons for these changes are the reduction in cropland and grassland areas and the increase in forestland and built-up area.

Figures 6 to 8 illustrate the changes in evapotranspiration, groundwater recharge, and surface runoff depth under different land use scenarios at the spatial scale. As shown in Figure 6, from 1985 to 2005, changes in land use types in the Da Wen River Basin resulted in increased evapotranspiration in most sub-basins, with only a small area in the northeast showing a decrease in evapotranspiration. From 2005 to 2021, a decrease in evapotranspiration was observed in the western and marginal areas of the basin, accounting for approximately 30% of the basin area. The overall increase in evapotranspiration during the entire study period was mainly influenced by the period from 1985 to 2005.

From Figures 7 and 8, it can be observed that from 1985 to 2021, changes in land use in the basin resulted in a decrease in groundwater recharge in all sub-basins, with an increase in surface runoff depth in all sub-basins except for a small area in the northeast. There is a consistent and negative correlation between the changes in groundwater recharge and surface runoff depth across the spatial distribution. The sub-basins with the greatest decrease in groundwater recharge are also the ones with the greatest increase in surface runoff depth. In this basin during the study period, there was a continuous reduction in arable land area and a significant expansion of built-up land, with an increase of up to 215%. In Figure 7(b), there is an increase in groundwater recharge in some sub-basins in the central and southwestern marginal areas of the basin, mainly due to an increase in water body area in these regions. In Figure 8, a decrease in surface runoff depth is observed in a small area in the northeast, primarily due to an increase in forest area in this

region, which increases surface roughness and prolongs the duration of surface water infiltration, thereby reducing surface runoff.

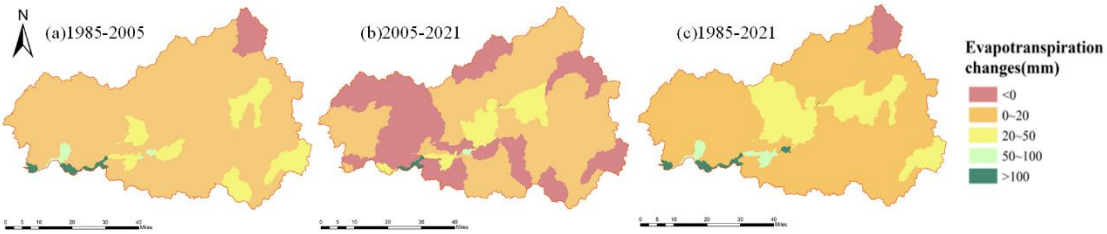

Figure 6. The spatial distribution of changes in basin evapotranspiration

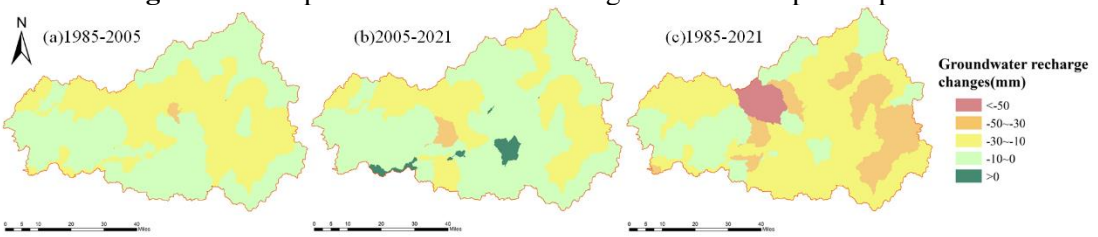

Figure 7. The spatial distribution of changes in basin groundwater recharge

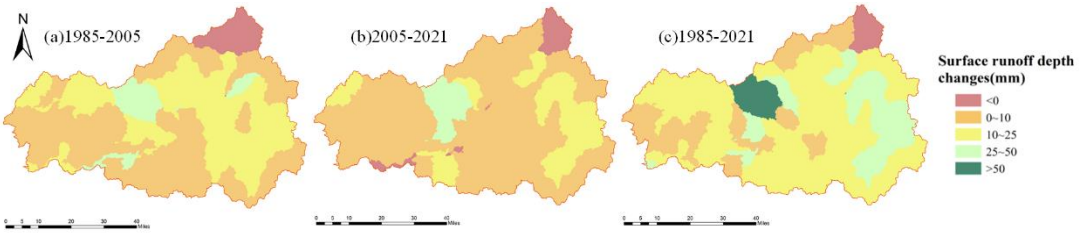

Figure 8 The spatial distribution of changes in basin surface runoff depth

Multi-objective decision tree analysis in the Random Forest algorithm quantifies the effects of different land use types on surface runoff depth to analyze the correlation between the two. Using the watershed land use type as the independent variable, considering the hydrological response unit and sub-watershed division, inputting the random forest regression model, the top three land use types that affect the surface runoff depth were calculated to be cropland, forest land, and grassland, with relative importance weight coefficients of 1.0729, 0.9607, and 0.8305, respectively.

Discussion

From the results of the analysis in section 3.1 of this paper, it can be seen that the SWAT model has good applicability in the Dawen River Basin, but there is a large gap between the simulation results and the measured values during the peak summer runoff period, as shown in Figure 2. Most of the peak flows appear to be underestimated, which is similar to the results of many other studies on the application of the SWAT model[42]. This error is accepdigle due to the complexity of hydrologic modeling principles and the inherent uncertainty in model calibration. It is important to note that the SWAT model is not calibrated for single-event high flow conditions. Therefore, some discrepancies between simulated and measured values, particularly during peak summer runoff periods, are expected and can be considered reasonable.

[43]. However, limitations in the model's ability to capture peak flows and low flows can affect the extreme values of surface runoff [44]， if this hydrologic model is used to quantify the impacts of different land use scenarios on surface runoff, the magnitude of the impacts may be misestimated. But the effect of the model's ability to capture peak flows on the surface runoff LUCC response was not considered in this study and will be further explored in future studies.

Drivers of land use change mainly include natural drivers (e.g., geomorphology, natural disasters) and socio-economic drivers (e.g., population growth, industrial development, government behavior)[45,46]. Natural drivers are relatively stable and have a cumulative effect, while socio-economic drivers are relatively dynamic and have a direct impact on land use change [47,48].

In the process of human development, to meet the needs of production and life, people's development and utilization of land have changed the type and distribution of local land use. The total population of Tai'an City was 4.733 million in 1985, and by 2021, the city's total population is projected to reach 5.435 million, with a population increase of 702,000 over 37 years. The increase in population in the watershed has caused changes in the land use pattern of the Dawen River Basin, with the area of built-up land expanding. Policy factors are one of the key drivers of changes in land use types in the short term. The 1987 "Tai'an Forestry Zoning" stipulates that the construction of mountainous areas should focus on water-sourcing and nutrient forests, leading to an increase in the planting area of forested land. The 2006 "Laiwu Municipal Land Use Overall Planning" emphasizes optimizing the spatial pattern of land use, strengthening control over land use in the central urban area, protecting agricultural land, promoting the construction of basic agricultural land, and encouraging the conservation and intensive use of built-up land. These policies have played a significant role in controlling land use changes.

The land use data from 1985 and 2021 were applied to the Land Expansion Analysis Strategy (LEAS) module of the PLUS model to simulate and calculate the contribution of driving factors to land use changes in each land use type in the Dawen River Basin. The results are shown in Figure 8. From the figure, it can be observed that the main drivers of cropland expansion in the Dawen River Basin are GDP, temperature, and precipitation. Woodland expansion is mainly driven by GDP, temperature, and slope. Grassland expansion is primarily influenced by slope and distance from roads. Watershed expansion is driven by distance from watershed and precipitation, while impervious surface expansion is influenced by distance from watershed, population, and slope.

Evapotranspiration is an essential component of the water cycle and serves as the link between the water and energy cycles. [49,50]. In this study, during the analysis of the response of hydrologic elements to changes in land use types, a significant trend of increasing evapotranspiration in the watershed was observed. Since the 1980s, China's climate and subsurface elements have undergone significant changes, most notably characterized by a sustained rise in temperature and widespread greening of vegetation[51]. Under the influence of climate and subsurface elements, many studies have shown that terrestrial evapotranspiration in China is increasing significantly[14,52]. This is consistent with the findings of this paper. However, the reduction of vegetation due to the decrease in the area of cultivated land and grassland, and the increase in the area of impervious surface due to the expansion of construction land in the Dawen River Basin from 1985 to 2021 are factors that inhibit evapotranspiration from the basin, which is inconsistent with the simulation results. Controversy still exists about the impact of land use changes on hydrological processes.

The regulatory role of the same land use varies from one watershed to another due to prevailing spatial heterogeneity in climate and subsurface conditions. For example, it has been argued that increased woodland and grassland cover can effectively reduce flood peaks and flood volumes, some scholars have

argued that an increase in woodland will lead to an increase in flooding. Chen et al[53] argued that the effect of vegetation cover on soil moisture content is still highly controversial due to the strong transpiration and interception of vegetation. Under dense vegetation, soil moisture may be reduced. Conversely, an increase in canopy vegetation shades the soil surface, reducing direct radiation uptake, which leads to a decrease in soil temperatures and evaporation rates, gradually increasing soil moisture. Li et al [54] found that compared to cropland, forests have a greater capacity for rainfall harvesting and water absorption, and therefore produce lower water yields, which is in line with previous findings by Yang[55]. However, Li et al.[46] showed that the shrinking of the woodland would lead to a gradual decrease in soil moisture, contributing to a slight increase in runoff during the dry period. Therefore, the effect of vegetation cover on soil moisture is complex, with both positive and negative effects, and requires in-depth investigation of the mechanisms of its influence.

The hydrological processes in the region are influenced by the combination of climatic and subsurface elements, resulting in a high degree of spatial and temporal heterogeneity. The trends in hydrological processes and the results of attribution of dominant factors obtained from different studies vary widely. Due to the limitations of data and model structure, this study only considered the land use change scenarios, without fully excluding the impacts of climate change and human activities on hydrological elements. This approach has certain limitations. It is important to comprehensively consider the impacts of hydrological elements, including climatic conditions, human activities, and spatial heterogeneity of the watershed, in order to conduct a more comprehensive study on the changes of hydrological elements in the watershed and the attribution of the evolution of hydrological processes. This will be the focus of subsequent work.

References

.

1 Tsihrintzis, V. A. & Vangelis, H. Water Resources and Environment. *Water Resources Management* **32**, 4813-4817 (2018).

2 Montanari, A. *et al.* "Panta Rhei—Everything Flows": Change in hydrology and society—The IAHS Scientific Decade 2013–2022. *International Association of Scientific Hydrology Bulletin*.

3 Blschl, G., Bierkens, M. F. P., Chambel, A., Cudennec, C. & Zhang, Y. Twenty-three unsolved problems in hydrology (UPH) – a community perspective. *Hydrological Sciences Journal/Journal des Sciences Hydrologiques* **64**, 1141-1158 (2019).

4 Moran-Tejeda, E., Ceballos-Barbancho, A. & Llorente-Pinto, J. M. Hydrological response of Mediterranean headwaters to climate oscillations and land-cover changes: The mountains of Duero River basin (Central Spain). *Global & Planetary Change* **72**, 39-49 (2010).

5 Yang, Q. *et al.* Hydrological Responses to Climate and Land-Use Changes along the North American East Coast: A 110-Year Historical Reconstruction. *Jawra Journal of the American Water Resources Association* **51**, 47-67 (2015).

6 Yao, T. *et al.* Third Pole Environment (TPE). *Environmental Development* (2012).

7 Fan, M. & Shibata, H. Simulation of watershed hydrology and stream water quality under land use and climate change scenarios in Teshio River watershed, northern Japan. *Ecological Indicators* **50**, 79-89 (2015).

8 Geng, L. J. Soil resistance to runoff on steep croplands in Eastern China. *Catena: An Interdisciplinary Journal of Soil Science Hydrology-Geomorphology Focusing on Geoecology and Landscape Evolution* **152** (2017).

9 Lin, J. *et al.* Flow-driven soil erosion processes and the size selectivity of eroded sediment on steep slopes using colluvial deposits in a permanent gully. *Catena* **157**, 47-57 (2017).
10 Keesstra, S., Nunes, J., Novara, A., Finger, D. & Cerdà, A. The superior effect of nature based solutions in land management for enhancing ecosystem services. *Science of the Total Environment* **610-611**, 997 (2017).
11 Gashaw, T., Tulu, T., Argaw, M. & Worqlul, A. W. Modeling the hydrological impacts of land use/land cover changes in the Andassa watershed, Blue Nile Basin, Ethiopia. *Science of The Total Environment* **619**, 1394 (2018).
12 Marhaento, H., Booij, M. J., Rientjes, T. H. M. & Hoekstra, A. Y. Attribution of changes in the water balance of a tropical catchment to land use change using the SWAT model. *Hydrological Processes* **31**, 2029-2040 (2017).
13 Warburton, M. L., Schulze, R. E. & Jewitt, G. P. W. Hydrological impacts of land use change in three diverse South African catchments. *Journal of Hydrology* **414**, 118-135 (2012).
14 Shujiang, P., Xiaoyan, W., Melching, C. S. & Feger, K. H. Development and testing of a modified SWAT model based on slope condition and precipitation intensity. *Journal of Hydrology* **588**, 125098 (2020).
15 Bosch, J. M. & Hewlett, J. D. A review of catchment experiments to determine the effect of vegetation changes on water yield and evapotranspiration. *Journal of Hydrology* **55**, 3-23 (1982).
16 Li, H., Zhang, Y., Vaze, J. & Wang, B. Separating effects of vegetation change and climate variability using hydrological modelling and sensitivity-based approaches. *Journal of Hydrology* **420**, 403-418 (2012).
17 Mwangi, H. M., Julich, S., Patil, S. D., Mcdonald, M. A. & Feger, K. H. Modelling the impact of agroforestry on hydrology of Mara River Basin in East Africa. *Hydrological Processes* **30**, 3139-3155 (2016).
18 Li, Z., Liu, W., Zhang, X. & Zheng, F. Impacts of land use change and climate variability on hydrology in an agricultural catchment on the Loess Plateau of China. *Journal of Hydrology* **377**, 35-42 (2009).
19 Devi, G. K., Ganasri, B. P. & Dwarakish, G. S. in *International Conference on Water Resources, Coastal and Ocean Engineering.*
20 Wang, G., Yang, H., Wang, L., Xu, Z. & Xue, B. Using the SWAT model to assess impacts of land use changes on runoff generation in headwaters. *Hydrological Processes* **28**, 1032-1042 (2014).
21 Waseem, M., Kachholz, F., Jens, T. R. & NCKNER. Suitability of common models to estimate hydrology and diffuse water pollution in North-eastern German lowland catchments with intensive agricultural land use. *Frontiers of Agricultural Science and Engineering* **5** (2018).
22 Gassman, P. W., Sadeghi, A. M. & Srinivasan, R. Applications of the SWAT Model Special Section: Overview and Insights. *Journal of Environmental Quality* **43** (2014).
23 SWAT: model use, calibration, and validation. (Special Issue: Model use, calibration, and validation.). *Transactions of the ASABE* (2012).
24 Manoj *et al.* Assessing SWAT models based on single and multi-site calibration for the simulation of flow and nutrient loads in the semi-arid Onkaparinga catchment in South Australia. *Agricultural Water Management* (2016).
25 Baker, T. J. & Miller, S. N. Using the Soil and Water Assessment Tool (SWAT) to assess land use impact on water resources in an East African watershed. *Journal of Hydrology* **486**, 100-111 (2013).
26 Zhang, H. *et al.* Using an improved SWAT model to simulate hydrological responses to land use change: A case study of a catchment in tropical Australia. *Journal of Hydrology* **585** (2020).
27 Zhang, Q. Influence of Land Use Change on Hydrological Cycle: Application of SWAT to Su-Mi-Huai Area in Beijing, China. *Water* **12** (2020).

28 Hu, J., YipingWang, LijingSun, PengchengZhao, FuboJin, ZhangdongWang, YunqiangQiu, LinjingLian, Yanqing. Impacts of land-use conversions on the water cycle in a typical watershed in the southern Chinese Loess Plateau. *Journal of Hydrology* **593** (2021).

29 Li, M. & Shao, Q. An improved statistical approach to merge satellite rainfall estimates and raingauge data. *Journal of Hydrology* **385**, 51-64 (2010).

30 Tran, A. P., Bogaert, P., Wiaux, F. O., Vanclooster, M. & Lambot, S. High-resolution space–time quantification of soil moisture along a hillslope using joint analysis of ground penetrating radar and frequency domain reflectometry data. *Journal of Hydrology* **523**, 252-261 (2015).

31 Arnold, J. G. & Allen, P. M. AUTOMATED METHODS FOR ESTIMATING BASEFLOW AND GROUND WATER RECHARGE FROM STREAMFLOW RECORDS1. *JAWRA Journal of the American Water Resources Association* **35**, 411-424 (1999).

32 Arnold, J. G. & Fohrer, N. SWAT2000: current capabilities and research opportunities in applied watershed modelling. *Hydrological Processes* (2005).

33 Abbaspour. SWAT-CUP 2012: SWAT Calibration and Uncertainty Programs - A User Manual. (2014).

34 Abbaspour, K. C. *et al.* Modelling hydrology and water quality in the pre-alpine/alpine Thur watershed using SWAT. *Elsevier* (2007).

35 Beven, K. J. The future of distributed models : Model calibration and uncertainty prediction. *Hydrol. Processes* **6** (1992).

36 Zhang, J., Li, Q., Guo, B. & Gong, H. The comparative study of multi-site uncertainty evaluation method based on SWAT model. *Hydrological Processes* **29**, 2994-3009 (2015).

37 Van Griensven, A. & Bauwens, W. Multiobjective autocalibration for semidistributed water quality models. *Water Resources Research* **39**, - (2003).

38 Marshall, L., Nott, D. & Sharma, A. A comparative study of Markov chain Monte Carlo methods for conceptual rainfall-runoff modeling. *Water Resources Research* **40**, 183-188 (2004).

39 Yang, J., Reichert, P., Abbaspour, K., Xia, J. & Yang, H. Comparing uncertainty analysis techniques for a SWAT application to the Chaohe Basin in China. *Journal of Hydrology* **358**, 1-23 (2008).

40 Geza, M. & Mccray, J. E. Effects of soil data resolution on SWAT model stream flow and water quality predictions. *Journal of Environmental Management* **88**, 393-406 (2008).

41 Dongwen, C. & Rong, G. Random Forest Prediction Model and Its Application to Hydrology Based on Random Drift Particle Swarm Optimization. *Journal of China Three Gorges University(Natural Sciences)* (2019).

42 Saha, P. P., Zeleke, K. & Hafeez, M. Streamflow modeling in a fluctuant climate using SWAT: Yass River catchment in south eastern Australia. *Environmental Earth Sciences* **71**, 5241-5254 (2014).

43 Zhang, H., BinLiu, De LiZhang, MingxiFeng, PuyuCheng, LeiYu, QiangEamus, Derek. Impacts of future climate change on water resource availability of eastern Australia: A case study of the Manning River basin. *Journal of Hydrology* **573** (2019).

44 Tessema, S. M., Lyon, S. W., Setegn, S. G. & Mrtberg, U. Effects of Different Retention Parameter Estimation Methods on the Prediction of Surface Runoff Using the SCS Curve Number Method. *Water Resources Management* **28**, 3241-3254 (2014).

45 Dang, A. N. & Kawasaki, A. Integrating biophysical and socio-economic factors for land-use and land-cover change projection in agricultural economic regions. *Ecological Modelling* **344**, 29-37 (2017).

46 Li, Y. *et al.* Spatiotemporal impacts of land use land cover changes on hydrology from the mechanism perspective using SWAT model with time-varying parameters. *Nordic Hydrology* (2019).

47 Hualin, X., Qu, L. & Guiying, L. Evolution characteristics and driving forces of wetland changes in the Poyang Lake eco-economic zone of China. *Scientific Research & Essays* **9**, 24-34 (2014).

48 P. *et al.* Land-cover and land-use change in a Mediterranean landscape: A spatial analysis of driving forces integrating biophysical and human factors. *Applied Geography* **28**, 189-209 (2008).
49 Jung, M. *et al.* Recent decline in the global land evapotranspiration trend due to limited moisture supply. *Nature*.
50 Fisher, J. B. *et al.* The future of evapotranspiration: Global requirements for ecosystem functioning, carbon and climate feedbacks, agricultural management, and water resources. *Water Resources Research* **53** (2017).
51 Zhu, Z. *et al.* Greening of the Earth and its drivers. *Nature Climate Change* (2016).
52 Bai, P., Liu, X., Zhang, Y. & Liu, C. Assessing the Impacts of Vegetation Greenness Change on Evapotranspiration and Water Yield in China. *Water Resources Research* **56** (2020).
53 Chen, X., Zhang, Z., Chen, X. & Shi, P. The impact of land use and land cover changes on soil moisture and hydraulic conductivity along the karst hillslopes of southwest China. *Environmental Earth Sciences* **59**, 811-820 (2009).
54 Li, L. *et al.* Responses of LAI to rainfall explain contrasting sensitivities to carbon uptake between forest and non-forest ecosystems in Australia. *Scientific Reports* **7**, 11720 (2017).
55 Yang, K. & Lu, C. Evaluation of land-use change effects on runoff and soil erosion of a hilly basin — the Yanhe River in the Chinese Loess Plateau. *Land Degradation & Development* (2018).

Data availability

The ASTER GDEM data set is available at http://www.gscloud.cn.Shandong Land Use Current Remote Sensing Monitoring Data is available at http://www.resdc.cn.Chinese Soil Type Spatial Distribution Data is available at http://dx.doi.org/10.3334/ORNLDAAC/1247.Chinese Meteorological Assimilation Drive Datase is available at https://doi.org/10.3972/westdc.002.2016.db. https://cstr.cn/18406.11.westdc.002.2016.db.

Hydrological Station Monthly Scale Runoff Data is available from the corresponding author on reasonable request.

Funding

This research was funded by Natural Science Foundation of Shandong Province, grant numbers ZR202102220203.

Author contributions statements

G.W. planned and supervised the project. Y.D., Z.F., J.Z., Y.L. and X.Q. analyzed the data and performed simulations. Y.L. wrote the main manuscript text. All authors reviewed the manuscript

Competing interests

The authors declare no competing interests.